Table 3 Mating tests between the selected line and original Keele stock

Nos of matings and estimates of preferences

Stocks and sexes used in matings	Nos of matings between different phenotypes Q×Q	Q×T	T×Q	T×T	Estimates of preference for Q $\hat{\gamma} \pm \sqrt{\text{var}(\hat{\gamma})}$
Selected ♂♂ × Keele ♀♀	11	28	17	34	0.1905 ± 0.0746
Selected ♀♀ × Keele ♂♂	16	28	6	15	0.5385 ± 0.0829
Keele ♂♂ × Keele ♀♀	18	35	21	42	0.2241 ± 0.0661

Analysis of χ^2

Component of variation	Value of χ^2	d.fs	Value of P
Selected males compared with Keele males	0.1126	1	0.737
Selected females compared with Keele females	10.4844	1	0.00120

The selected males and females used in these tests were taken from the progeny of the fourth generation of the selected line. No further selection had been imposed after the fourth generation. The level of preference among the progeny of the fourth generation should be the same as that in the fourth generation. The selected males and females were tested in matings with progeny taken from the corresponding generation of the original Keele stock. Population cages were set up with 7:3 ratios of T:Q. They were kept under continuous observation; mating pairs were counted giving the numbers shown in the table.

The response to selection that we have demonstrated has taken place in the females' mating preference for *quadrimaculata* males. As shown in Table 3, when selected females are mated with males from the original stock, the level of preference is characteristic of the selected line; when selected males are mated with females from the original stock, the level of preference is characteristic of the original stock. Female mating preference has thus been shown to have a large genetic component in its determination. We believe that these experiments provide the first formal proof that a female mating strategy is genetically determined.

This proof is fundamental for theories of the evolution of female preference[4–7]. It shows that female choice of mate can evolve: mate choice will be selected if, as in our experiment, females making the choice contribute a relatively greater proportion of offspring to future generations. In a natural population, they will do so if the males they choose to mate with possess a selective advantage. As the female preference contributes some of this selective advantage, it partly selects itself. This gives rise to what Fisher[4] called the 'runaway process of sexual selection'. Initially, while preference genes are rare—they may perhaps have arisen by mutation—this process will be extremely slow, requiring many thousands of generations to get started[5]. Realistically, male competition or natural selection must provide the initial advantage. The preference will then be selected in the course of the selection of the preferred male character. The dynamics of this selection is very complex and depends crucially on the genetics of the preference[5]. Initially, as a gene for the preferred character spreads through a population, a preference gene may be expected to show a three- to fivefold increase in frequency. As the preference becomes more common, it adds to the preferred males' advantage; but the preference gene itself shows progressively smaller increases in frequency as it becomes more common. The process eventually stops when the male character has developed to the point at which it has become so disadvantageous in natural selection that this disadvantage balances the sexual selection.

This work was supported by a research grant from the SERC to P. O'D.

Received 23 August; accepted 25 October 1982.

1. Lewontin, R. C. *Nature* **266**, 283–284 (1977).
2. Dawkins, R. *The Selfish Gene* (Clarendon, Oxford, 1976).
3. Darwin, C. *The Descent of Man and Selection in Relation to Sex* (Murray, London, 1871).
4. Fisher, R. A. *The Genetical Theory of Natural Selection* (Clarendon, Oxford, 1930).
5. O'Donald, P. *Heredity* **22**, 499–518 (1967).
6. O'Donald, P. *Genetic Models of Sexual Selection* (Cambridge University Press, 1980).
7. Lande, R. *Proc. natn. Acad. Sci. U.S.A.* **78**, 3721–3725 (1981).
8. Muggleton, J. *Heredity* **42**, 57–65 (1979).
9. Muggleton, J. & O'Donald, P. *Heredity* **43**, 143–148 (1979).
10. Majerus, M. E. N., O'Donald, P. & Weir, J. *Heredity* **49**, 37–49 (1982).
11. Lus, J. J. *Trudy Lab. Genet.* **9**, 135–162 (1932).
12. Karlin, S. & O'Donald, P. *Heredity* **41**, 165–174 (1978).
13. O'Donald, P. *Heredity* **44**, 309–320 (1980).
14. O'Donald, P. *Nature* **272**, 189 (1978).

Phenomenal coherence of moving visual patterns

Edward H. Adelson* & J. Anthony Movshon

Department of Psychology, New York University, New York, New York 10003, USA

When a moving grating is viewed through an aperture, only motion orthogonal to its bars is visible, as motion parallel to the bars causes no change in the stimulus. Because there is a family of physical motions of various directions and speeds that appear identical, the motion of the grating is ambiguous. In contrast, when two crossed moving gratings are superimposed, the resulting plaid pattern usually moves unambiguously and predictably. In certain cases, however, two gratings do not combine into a single coherent percept, but appear to slide across one another. We have studied the conditions under which coherence does and does not occur, and we report here that it depends on the relative contrasts, spatial frequencies and directions of motion of the gratings. These effects may reveal the previously unstudied properties of a higher order stage of motion analysis.

Figure 1*a* illustrates the problem of ambiguity[1,2]. The grating moves behind a circular aperture. Any of the physical motions indicated by the arrows will appear the same when viewed through the aperture. The situation can be depicted graphically in 'velocity space', a space in which each vector represents a velocity: the length of a vector corresponds to speed, and its angle corresponds to direction. As shown in Fig. 1*a*, the motion of a single grating is consistent with a family of motions that lies along a line in velocity space; this line is parallel to the grating's bars and orthogonal to the vector representing its 'primary' motion. If two moving gratings are superimposed, the resulting 'plaid' pattern moves with a speed and direction which can be exactly predicted from the velocity space construction: the two loci of possible motions intersect at a single point, corresponding to the motion of the coherent pattern (Fig. 1*b*). This solution to the 'aperture problem' is similar to that proposed (in a rather different context) by Fennema and Thompson[3]. It has advantages over that advanced by Marr and Ullman[4], which can only infer a range of possible directions from the limited information provided by a pair of gratings.

The velocity space combination rule is also different from a vector sum or vector average. In Fig. 1*c*, two gratings move downward and rightward with different speeds and directions.

* Present address: RCA David Sarnoff Research Center, Princeton, New Jersey 08540, USA.

0028–0836/82/490523—03$01.00

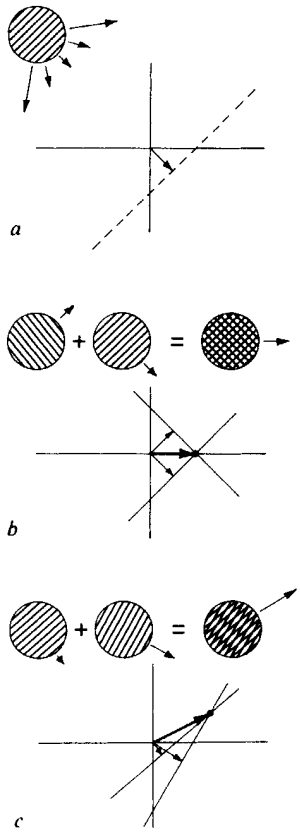

Fig. 1 The velocity-space representation of some moving patterns. In each panel, a vector represents a motion in a direction given by the vector's angle at a speed given by the vector's length. *a*, A single grating moves behind an aperture. The broken line indicates the locus of velocities compatible with the motion of the grating. *b*, A plaid composed of two orthogonal gratings moving at the same speed. The lines give the possible motions of each grating alone. Their intersection is the only shared motion, and corresponds to what is seen. *c*, A plaid composed of two oblique gratings, one moving slowly and the other more rapidly. Both gratings move down and to the right, but the pattern moves up and to the right.

A vector sum or average would predict a pattern motion that was also downward and rightward, but the velocity space solution is a motion upward and rightward, the motion that observers report when the gratings are seen to cohere[5]. Of course, nothing requires that coherent motion be seen, and instead of a single rigidly moving plaid, the two gratings are sometimes seen sliding 'incoherently' over each other. We have studied the stimulus conditions under which coherence occurs, in order to characterize the mechanisms that underly the coherent percept and resolve the ambiguity of one-dimensional motion.

Observers viewed a circular cathode ray tube display subtending 5°; the luminance of the display was constant on average, but was modulated by signals from a PDP11 computer to produce a superimposed pair of sinusoidal gratings that could each be varied in orientation, direction and speed of motion, contrast and spatial frequency. Observers were strictly instructed not to make judgements unless their eyes were steadily fixated on a small black circle in the centre of the display. Subjects under this kind of instruction are capable of stable and reliable fixation[6]. After each 1.5-s exposure, the observer indicated whether the pattern appeared 'coherent' or 'incoherent'.

Contrast strongly affects coherence, even when both gratings are easily visible. Figure 2*a* shows a psychometric function for detection and a similar function for coherence, when the contrast of one of the gratings in a plaid was varied (the other grating's contrast was fixed at 0.3). The gratings were of the same spatial frequency, and moved at an angle of 135° to one another. Open symbols show the probability of detecting the low-contrast grating in the presence of its high-contrast mate. Filled symbols show the probability of a coherent percept. Both detection and coherence become more likely as contrast increases, but reliable coherence only occurs at contrasts where both gratings are clearly visible.

In further experiments, we used this contrast dependence to measure the relative tendency of different pairs of gratings to cohere. We fixed the contrast of one grating at 0.3, and used a staircase procedure to vary the contrast of the other grating until the observer saw coherent motion on half the trials. The gratings' speed, orientation and spatial frequency all affected the strength of coherence. Coherence decreased as the speed of the component gratings increased, as the angle between their 'primary' directions increased, and as the difference between their spatial frequencies increased.

Figure 2*b* shows the effect of relative spatial frequency on coherence. Filled symbols illustrate a case in which the spatial frequency of the high-contrast grating was fixed at 1.2 cycles deg^{-1}, while the spatial frequency and contrast of the second grating were varied; open symbols illustrate a case where the spatial frequency of the first grating was fixed at 2.2 cycles deg^{-1}. As the frequencies of the two gratings were made different, the tendency to cohere was reduced, and the contrast needed for coherence was increased. This spatial frequency dependence suggests that coherent motion, like many other visual properties, is analysed by mechanisms that are selective for spatial frequency.

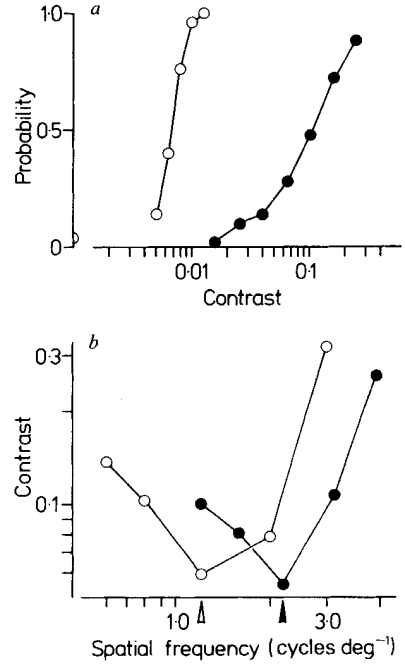

Fig. 2 Two parameters influencing perceptual coherence. *a*, The influence of contrast on the detectability and coherence of two crossed sinusoidal gratings. One grating was fixed in contrast at 0.3. The other was of variable contrast, and moved at an angle of 135° to the first; both had a spatial frequency of 1.6 cycles deg^{-1}, and moved at 3 deg s^{-1}. Filled symbols show the probability that the observer judged the two gratings to be 'coherent'; open symbols show the probability that the observer detected the presence of the lower contrast grating. The half-circle on the ordinate shows the probability that the observer judged the second grating to be present when its contrast was zero—the 'false-positive rate' for detection; the false-positive rate for coherence judgments was zero. Subject, E.H.A. *b*, The influence of spatial frequency on coherence. The standard grating again had a contrast of 0.3 and moved at 3 deg s^{-1}. The test gratings moved at an angle of 135° to the standard, also at 3 deg s^{-1}. Open symbols show the results for a range of test spatial frequencies when the standard grating had a spatial frequency of 1.2 cycles deg^{-1} (open arrow). Filled symbols show the results when the standard grating had a spatial frequency of 2.2 cycles deg^{-1} (filled arrow). Subject, P.A.

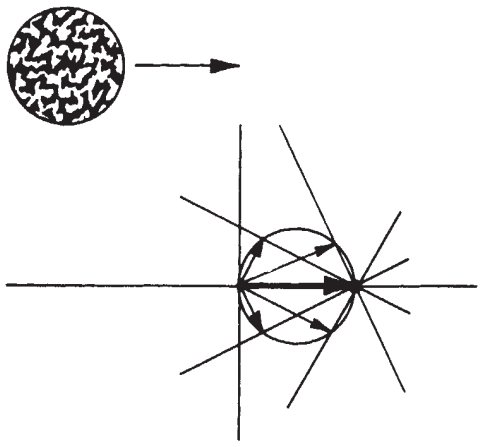

Fig. 3 The velocity-space representation of a random-texture field moving to the right. The field contains components of all orientations, and the primary motion vector for each ends on the circle passing through the origin; the common motion 'implied' is the rightward motion given by the bold arrow. This circular locus of primary motions represents all the motions that can exist in a single rightward-moving pattern. As such, the locus could represent the preferences of a family of primary motion analysers whose outputs are combined to signal coherent two-dimensional motion (see text).

There are two kinds of model that might account for our results. The first relies on the presence in our patterns of localizable blob-like features where the peaks and troughs of the crossed gratings intersect. Some process based on direction-selective elements not selective for orientation might detect and signal the motion of these 'blobs', which is of course identical to the motion of the pattern as a whole. We have evidence to suggest that such a scheme is incorrect. We superimposed one-dimensional dynamic random visual noise (a rapidly changing pattern of random-width lines)[7] on our test patterns. A non-oriented mechanism that responds directly to the motion of blobs should be most affected by noise oriented at right angles to the coherent motion. But a mechanism that combines the outputs of oriented channels should be most affected when those channels are most affected—when the noise is oriented at right angles to the primary motion of one or the other of the component gratings. Our results support the orientation-based model. Coherence is strongly reduced when the noise mask is perpendicular to a component's motion (and thus parallel to the component's orientation), but is almost unaffected when the mask is perpendicular to the coherent motion of the pattern. This suggests that some orientation-selective process must precede the analysis of coherent motion, and our second model incorporates this feature.

There is abundant evidence that visual analysing mechanisms selective for orientation and spatial frequency exist at a relatively early stage in the visual pathway[8–12]. It is clear that such mechanisms are often sensitive to the direction of motion of one-dimensional contours[8,9,13–15], but they also seem unable to signal the true direction of motion of two-dimensional patterns[16–19]. The perceptual coherence of two gratings into a single moving plaid may therefore represent the action of an additional stage of visual processing beyond those usually considered to be involved in analysing motion. At this second stage, the outputs of several 'one-dimensional' motion analysers would be combined. Coherence phenomena may offer an approach to studying the properties of this postulated second-stage motion analyser.

Figure 3 shows how the velocity space construct helps to assign motion to more complex patterns, such as a horizontally moving random-texture field. The texture contains components of many orientations; their motions are represented in velocity space by the arrows in Fig. 3. As the speed of each component is proportional to the cosine of the angle between its direction and horizontal, the vectors all end on a circle that passes through the origin. Note also that the motion 'families' associated with the various components all pass through the common point corresponding to the horizontally directed pattern motion.

A given vector in Fig. 3 could represent the preference of a one-dimensional motion detector, and the circle might represent the 'receptive field' in velocity space of a second-stage motion analyser. If it combined the outputs of one-dimensional analysers corresponding to points on the circle by an operation akin to a logical 'and', the second-stage analyser would respond only to a particular direction of motion of the two-dimensional stimulus. Our results on perceptual coherence might reflect the relative strengths of the different inputs to such a motion analyser. They would suggest that this analyser computes the weighted combination of signals arising from a collection of one-dimensional motion analysers having different velocity preferences but similar spatial frequency preferences.

This work was supported by NIH grant EY 2017 to J.A.M. E.H.A. was supported by an NIH training grant (EY 7032) to New York University. J.A.M. holds a Research Career Development Award from NIH (EY 187), and was an Alfred P. Sloan Research Fellow in Neuroscience.

Received 18 July; accepted 7 October 1982.

1. Wohlgemuth, A. *Br. J. Psychol.* Monogr. Suppl. 1 (1911).
2. Wallach, H. *Psychol. Forsch.* **20**, 325–380 (1935).
3. Fennema, C. L. & Thompson, W. B. *Comp. Graph. Image Proc.* **9**, 301–315 (1979).
4. Marr, D. & Ullman, S. *Proc. R. Soc.* **B211**, 151–180 (1981).
5. Adelson, E. H. & Movshon, J. A. *J. opt. Soc. Am.* **70**, 1605 (1980).
6. Murphy, B. J., Kowler, E. & Steinman, R. M. *Vision Res.* **15**, 1263–1268 (1975).
7. Stromeyer, C. F. & Julesz, B. *J. opt. Soc. Am.* **62**, 1221–1232 (1972).
8. Hubel, D. H. & Wiesel, T. N. *J. Physiol., Lond.* **160**, 106–154 (1962).
9. Hubel, D. H. & Wiesel, T. N. *J. Physiol., Lond.* **195**, 215–243 (1968).
10. Robson, J. G. in *Handbook of Perception* (eds Carterette, E. C. & Friedman, M. P.) 81–116 (Academic, New York, 1975).
11. Campbell, F. W. & Robson, J. G. *J. Physiol., Lond.* **197**, 551–566 (1968).
12. Blakemore, C. & Campbell, F. W. *J. Physiol., Lond.* **203**, 237–260 (1969).
13. Henry, G. H., Bishop, P. O. & Dreher, B. *Vision Res.* **14**, 767–777 (1974).
14. Levinson, E. & Sekuler, R. *J. Physiol., Lond.* **250**, 347–366 (1975).
15. Watson, A. B., Thompson, P. G., Nachmias, J. & Murphy, B. *Vision Res.* **20**, 341–347 (1980).
16. Hammond, P. *J. Physiol., Lond.* **285**, 479–491 (1978).
17. De Valois, R. L., De Valois, K. K. & Yund, W. S. *J. Physiol., Lond.* **291**, 483–505 (1979).
18. Movshon, J. A., Davis, E. T. & Adelson, E. H. *Soc. Neurosci. Abstr.* **6**, 670 (1980).
19. Adelson, E. H. & Movshon, J. A. *Invest. Ophthalmol. Vis. Sci.* Suppl. **20**, 17 (1981).

Prenatal misrouting of the retinogeniculate pathway in Siamese cats

Carla J. Shatz & Michel Kliot

Department of Neurobiology, Stanford University School of Medicine, Stanford, California 94305, USA

In the mammalian visual system, retinal ganglion cells send their axons to several distinct structures in the brain. One of these, the lateral geniculate nucleus (LGN), receives a substantial projection from both eyes in higher mammals such as the cat[1–3]. How does this pattern of input arise during development? One possibility is that retinal ganglion cell axons project from the very beginning to the appropriate side of the brain. Another is that the initial projection may contain many inappropriate connections which are eliminated after the axons reach their target, the LGN. We thought the Siamese cat might provide an opportunity to study these alternatives. Guillery and others[4–7] have shown that in adult Siamese cats, the LGN receives a disproportionately large input from the contralateral eye and a correspondingly diminished input from the ipsilateral eye due to a genetic mutation at the *albino* locus. We report here that this abnormal pattern of input is present from the earliest stages of development of the retinogeniculate projection and arises as a consequence of the misrouting of fibres at the optic chiasm. These findings suggest that during normal development, growing optic fibres can be directed to the appropriate side of the brain.

0028–0836/82/490525—05$01.00